Magnon-drag Peltier effect in a Ni-Cu alloy*

G. N. Grannemann and L. Berger
Physics Department, Carnegie-Mellon University, Pittsburgh, Pennsylvania 15213
(Received 25 March 1975)

Peltier-effect measurements to an accuracy of 1% have been made on $Ni_{66}Cu_{34}$ and $Ni_{69}Fe_{31}$ at 1.3–4.2 K and magnetic fields to 5.5 T. The Peltier coefficient π is proportional to T^2 as expected for electron diffusion. However, the absolute value of π decreases by 7% in Ni-Cu and 4% in Ni-Fe when the field is increased from just above ferromagnetic saturation to 5.5 T, at 4.2 K. This decrease is consistent with a magnon-drag contribution to the Peltier coefficient, which is quenched by the field, at least in the case of Ni-Cu. The magnitude of the contribution, when combined with Hall data, indicates that the magnon gas drifts at a speed close to that of the 4*s* electron gas. Using a simple kinetic theory this implies that magnons relax faster on 4*s* electrons than on impurities. Interpretation of Ni-Fe data is not so clear.

I. INTRODUCTION

In an isothermal metal or semiconductor, an electric current density $\vec{j}$ is accompanied by a heat current density $\vec{Q}$, where $\vec{Q}=\pi\vec{j}$. The existence of $\vec{Q}$ constitutes the Peltier effect,[1,2] and the number π is called the Peltier coefficient. The absolute thermopower S of the material is related to π by the relation $S=\pi/T$.

The electrons contribute directly to the Peltier heat current, and this part is called the electron-diffusion contribution. If $T\ll T_F$, where T_F is the Fermi degeneracy temperature, then this part obeys $S=\pi/T\propto T$.

In a ferromagnet, the electron-diffusion Peltier effect usually depends somewhat on the angle between the direction of measurement and the saturation magnetization $\vec{M}_s$. This phenomenon is called ferromagnetic anisotropy of the Peltier effect or thermopower,[3] and is caused by spin-orbit interaction.

Because of electron-phonon collisions, the electric current may cause the phonon gas to have a nonequilibrium distribution and to drift with an average drift velocity $d\vec{v}_{ph}$. Then the phonon gas carries a nonzero heat current. This is the "phonon-drag" contribution[1,2] to the Peltier coefficient.

Bailyn and later authors[4] suggested that magnon-electron collisions would lead in conducting ferromagnets to a "magnon-drag" effect similar to phonon drag. The magnon gas would drift at a velocity $d\vec{v}_m$, and carry a nonzero heat current.

The present work is an attempt to find a magnon-drag contribution to the Peltier effect of a transition-series ferromagnet. In order to separate this contribution in a more convincing manner than could be achieved by earlier authors, we take advantage of the fact that magnons are quenched by a magnetic field. Moreover, we choose to make these measurements in a concentrated alloy, because we need to know that magnetic fields of order 5 T have a negligible effect on the electron-diffusion thermopower. These two important points of experimental technique, the necessity of which does not seem to be generally appreciated, have already been applied by us to the successful detection of a magnon contribution to the thermal conductivity of Ni-Fe alloys[5] and of Fe-Co alloys.[6]

Another simplifying feature of our experiments on alloys at low temperatures is the fact that electrons are scattered mostly by impurities. The existence of magnons has a negligible effect on the electron distribution.

An abstract on our present magnon-drag work has already been published.[7]

II. SIMPLE MAGNON-DRAG PELTIER THEORY

We assume a free-electron gas drifting at a velocity $d\vec{v}_e$ and a magnon gas drifting at a velocity $d\vec{v}_m$,

$$d\vec{v}_e=\vec{j}/n_e e\,,\quad d\vec{v}_m=\alpha_m d\vec{v}_e\,, \tag{1}$$

where α_m remains an adjustable parameter. Then the magnon distribution $n(\vec{q})$ is[8]

$$n(\vec{q})=n_0(E(\vec{q}-d\vec{q}))\simeq n_0(E(\vec{q}))-d\vec{q}\cdot\frac{\partial E}{\partial\vec{q}}\frac{dn_0}{dE}\,,$$
$$d\vec{q}=(\hbar/2D)\,d\vec{v}_m\,, \tag{2}$$

where n_0 is the Bose-Einstein distribution

$$n_0(E(\vec{q}))=\{\exp[E(\vec{q})/k_BT]-1\}^{-1}.$$

We write also for the magnon energy $E(\vec{q})$

$$E(\vec{q})=Dq^2+g\mu_B B_{\rm eff}\,,$$
$$x=Dq^2/k_BT\,,\quad y=g\mu_B B_{\rm eff}/k_BT\,. \tag{3}$$

The magnon heat flux in the x direction is

$$Q_x=\frac{1}{V\hbar}\sum_q n(\vec{q})E(\vec{q})\frac{\partial E}{\partial q_x}\,,$$

where V is the crystal volume.

Using Eqs. (1)–(3), this may be written

$$Q_x = \alpha_m \frac{j_x}{n_e e} \frac{(k_B T)^{5/2}}{6\pi^2 D^{3/2}} L(y), \qquad L(y) = \int_0^{+\infty} x^{3/2}(x+y) \frac{\exp(x+y)}{[\exp(x+y)-1]^2} dx. \tag{4}$$

Going back to the definition $\pi = Q_x/j_x$, Eqs. (4) give

$$S = \frac{\pi}{T} = \frac{\alpha_m}{n_e e} \frac{k_B^{5/2} T^{3/2}}{6\pi^2 D^{3/2}} L(y). \tag{5}$$

But the specific heat of the magnon gas per unit volume is,[9] at zero magnetic field,

$$C_m(B_{\text{eff}} = 0) = (k_B^{5/2} T^{3/2}/4\pi^2 D^{3/2}) L(0), \tag{6}$$

where $L(0) = 4.45$. Therefore

$$S = \frac{\pi}{T} = \frac{2\alpha_m}{3 n_e e} C_m(B_{\text{eff}} = 0) \frac{L(y)}{L(0)}. \tag{7}$$

The "quenching function" $L(y)/L(0) = L(y)/4.45$ has been calculated by numerical integration with a digital computer. The result is shown in Fig. 1.

The effective magnetic field B_{eff} appearing in Eqs. (3) is defined[10] in such a way as to include a part describing approximately the influence of dipole-dipole interaction on the dispersion relation $E(\vec{q})$ of magnons. In the case of a Peltier heat current flowing along a rod parallel to the external magnetic field $\vec{B}_E$ and to the saturation magnetization $\vec{M}_s$, one can show that in mks units

$$\vec{B}_{\text{eff}} = \vec{B}_E + \tfrac{7}{15}\vec{M}_s. \tag{8}$$

This expression is correct to first order in the parameter $j = g\mu_B M_s/k_B T$, and is valid only if $j \ll 1$. It is identical to the one derived by us[10] for the problem of thermal conduction by magnons, and is derived in a similar manner.

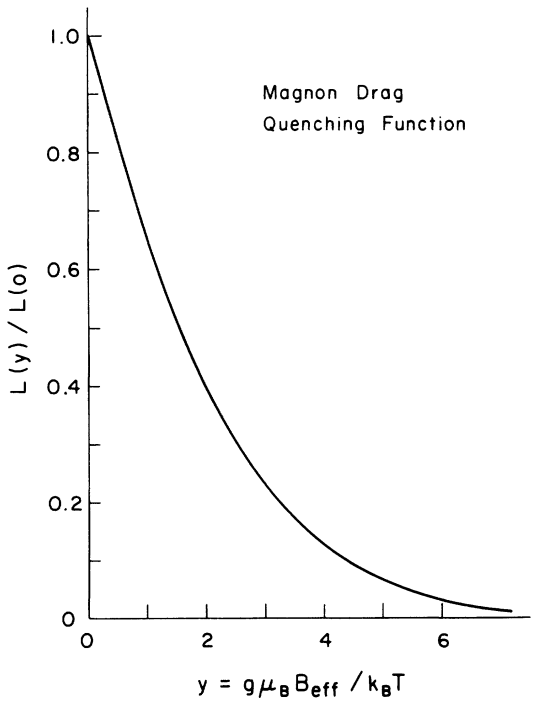

FIG. 1. Quenching function representing the influence of the effective field B_{eff} on the magnon-drag Peltier effect.

III. EXPERIMENTAL APPARATUS

Our apparatus for Peltier measurements is very similar to the ones of Fiory and Serin and of Trodahl,[11] though developed independently. The sample is in a can where the pressure is 2×10^{-6} Torr. The center of the cylindrical sample S is thermally connected to the liquid-helium bath through a clamp C made of tellurium copper (Fig. 2). Each end of the sample is soldered to a 0.25-mm-diam superconducting-alloy wire in order to provide the sample current I. These wires are brought to the liquid-helium bath through hollow glass-to-metal seals on the bottom of the vacuum can.

The two carbon thermometers R_1 and R_2 are 100-Ω, $\frac{1}{8}$-W Allen-Bradley resistors. Each one is glued inside a hole of a small copper block, which is clamped around the sample close to one end.

The two 300-Ω calibration heaters H_1 and H_2 are made of 0.025-mm-diam manganin wire, noninductively wound around pieces of lacquered No. 18 AWG copper wire which are soldered to the sample ends at the same point as the sample current wires (Fig. 2).

Each thermometer has two leads and each heater has four leads, made of a few cm of superconducting-alloy wire and manganin wire, followed by copper wires running to the top of the Dewar vessel through the vacuum line. These copper wires are thermally grounded to the helium bath by being wound around a copper post and glued to it.

The carbon thermometers R_1 and R_2 are connected to two adjacent arms of a Wheatstone bridge. The bridge circuit[12] allows us to measure R_1 directly in order to find the absolute sample temperature. It also allows us to determine $R_1 - R_2$ directly during Peltier measurements. This differential setting minimizes the effect of drifts of the bath temperature. At each magnetic field value, the thermometers are calibrated by measurements of the vapor pressure of the bath, in the absence of current through the sample.

The bridge is excited by a 33-Hz sine wave, and the bridge output is sent to a P.A.R. HR-8 lock-in amplifier. The rectified amplifier output is fed to a recorder. Using the differential setting of the bridge, and choosing well-matched carbon ther-

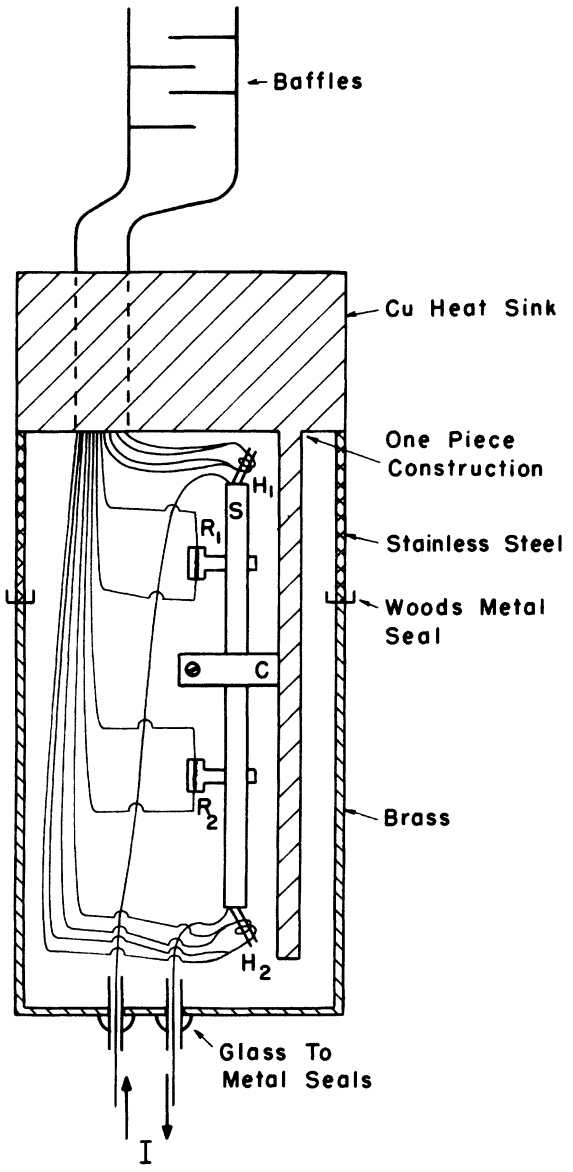

FIG. 2. Apparatus for measurements of the Peltier effect at low temperatures.

mometers, the recorder output during Peltier measurements depends mainly on the temperature difference $T_1 - T_2$ between the two thermometers.

The sample current I, of about 0.5–1 A, is provided by a current-regulated dc power supply and is measured by a digital voltmeter in parallel with a 1-Ω standard resistor.

The current feeding the calibration heaters H_1 and H_2 is provided by the voltage-regulated dc power supply PS_1 through a 1000-Ω sine-cosine potentiometer[13] acting as a voltage divider. One output voltage of the potentiometer is $V_0 \sin\alpha$ and the other is $V_0 \cos\alpha$, if the voltage across PS_1 is $2V_0$. Since $\sin^2\alpha + \cos^2\alpha = 1$, the sum of powers dissipated in H_1 and H_2 is nearly independent of the setting α of the potentiometer. The voltages across H_1 and H_2 are measured with a digital voltmeter. The voltages across 563-Ω standard resistors in series with H_1 and H_2 are also measured, in order to determine the current through the heaters.

The temperature of the liquid-helium bath is regulated by a mechanical manostat, together with an electronic regulator.[14]

The magnetic field is parallel to the electric current, and is provided by a superconducting magnet with 1% uniformity in a 25-mm-diam spherical volume.

In order to measure the electrical resistivity, the sample is immersed directly in the liquid-helium bath. The various clamps, thermometers, superconducting wires, and heaters are removed. Current leads are soldered to both ends of the sample. Two narrow phosphor-bronze voltage probes are clamped around the sample at the approximate former location of the thermometers. The ohmic voltages are measured with a Keithley Model 148 nanovoltmeter for both directions of the dc current, and averaged. The magnetic field is parallel to the current.

IV. PELTIER EXPERIMENTAL PROCEDURE

After the bath temperature is stabilized at the desired value, the sample current I is switched on, and set at a value such that the temperatures T_1 and T_2 of the thermometers do not differ from the bath temperature by more than 1%. A Peltier heat current πI is then flowing through the sample. Since the Peltier coefficient of the superconducting current leads (Fig. 2) is zero, a heat πI is taken from one end of the sample and an equal heat deposited at the other end every second. This causes a cooling of one end and a heating of the other end, and thus a small difference of temperature $T_1 - T_2$ exists. The sample current I is then reversed with a switch. This produces a reversal of $T_1 - T_2$ and therefore a change ΔX_{Pel} of the recorder output, which is measured. Note that a sizable joule heating of the sample is always present but is not affected by current reversal.

Then, in order to calibrate the recorder output directly in terms of power, the setting of the sine-cosine potentiometer is changed. This induces a change ΔH_1 of the power dissipated in calibration heater H_1, which is determined by heater voltage and current measurements. The change ΔH_2 of dissipation in H_2 is determined similarly. The sine-cosine potentiometer insures $\Delta H_1 \simeq -\Delta H_2$, simulating the Peltier effect in this respect. The average $\Delta H = \frac{1}{2}(|\Delta H_1| + |\Delta H_2|)$ is evaluated. The

corresponding change ΔX_{cal} of the recorder output is also measured.

Note that thermometer magnetoresistance or uncertainties in thermometer calibration do not affect the measured π values.

V. SAMPLE PREPARATION

The Ni-Cu alloy was made by melting together Johnson-Mathey metals in an induction furnace under a vacuum. It was swaged and machined to the shape of a cylinder 4.94 mm in diameter and 34.4 mm long. Then it was annealed in an electric furnace at 1090 °C for 25 h in a flow of dry hydrogen. The furnace was cooled to 900 °C, and the sample annealed for 3 h under a pressure of 5×10^{-6} Torr to remove the hydrogen. The furnace power was then shut off, and the sample allowed to cool to room temperature. The size of the crystal grains was about 0.5 mm. Wet chemical analysis indicated 36.03-wt% Cu, corresponding to $Ni_{66}Cu_{34}$.

Ni-Cu alloys have a tendency towards atomic clustering.[15] This clustering could be partially prevented by cooling the samples very rapidly after annealing; however, the properties of these alloys have been observed[16] to be slowly time dependent after such a quenching. Moreover, many existing physical data on Cu-Ni alloys, which we will use, have been obtained on unquenched samples. In a furnace-cooled sample such as ours, the effect of clustering is[17] only to increase by 12% the probability that a Ni atom will have other Ni atoms as nearest neighbors. Our $Ni_{66}Cu_{34}$ sample is a ferromagnet with a Curie point of $\simeq$250 K, and this Curie point is not[18] affected by clustering. Also, since we are rather far from the ferromagnetic critical concentration of 44-at% Ni, "magnetic polarization clouds"[19] should not exist in our sample. The Ni-Cu series remains very attractive for our investigations, despite its tendency towards clustering because the small value of its exchange stiffness D implies a large magnon-drag Peltier heat current [see Eq. (5)], and also because its physical characteristics are well known.

The Ni-Fe sample is one of those used by Yelon and Berger[5] to measure the contribution of magnons to the thermal conductivity. For our work, it was swaged and machined to the shape of a cylinder of diameter 4.79 mm and length 59.3 mm. Then it was annealed at 1250 °C for 24 h in a flow of dry hydrogen. The furnace was cooled to 900 °C and the sample was annealed for 2.5 h under a pressure of 5×10^{-5} Torr to remove the hydrogen. The furnace power was then shut off. Wet chemical analysis gives 29.81-wt% Fe, which corresponds to $Ni_{69}Fe_{31}$.

VI. Ni-Cu EXPERIMENTAL RESULTS

The Peltier coefficient π was measured as a function of temperature between 1.3 and 4.2 K for four different values of the external field: $B_E = 0$, 0.44, 2.2, and 4.4 T. We show the data for $B_E = 2.2$ T in Fig. 3, where $-\pi/T = -S$ is plotted against temperature. For the temperature T, we take the average of T_1 and T_2.

For the purpose of smoothing and interpolation, these data were fitted by least squares at each field to the empirical expression $\pi = A_1T + A_2T^2$, where A_1 and A_2 are adjustable constants. One example of the fit is shown in Fig. 3. We find A_1 to be very small, so that $\pi \propto T^2$ approximately, as expected if the electron-diffusion mechanism is dominant. However, $|\pi|$ decreases with increasing field by several percent. Considering only data above ferromagnetic saturation, we plot $S(B_E = 4.4\ \text{T}) - S(B_E = 0.44\ \text{T})$ and $S(B_E = 2.2\ \text{T}) - S(B_E = 0.44\ \text{T})$ versus temperature in Fig. 4, where $S = \pi/T$. These differences are calculated from the fitted empirical expressions.

The Peltier coefficient was also measured as a function of field, between $B_E = 0$ and $B_E = 6.4$ T, at a fixed temperature of 4.2 K. A pressure-sensitive bath-temperature regulator[20] was used there, rather than the Sommers regulator,[14] to prevent the magnetoresistance of the temperature sensor from causing temperature drifts. The temperature was not exactly the same on all three runs;

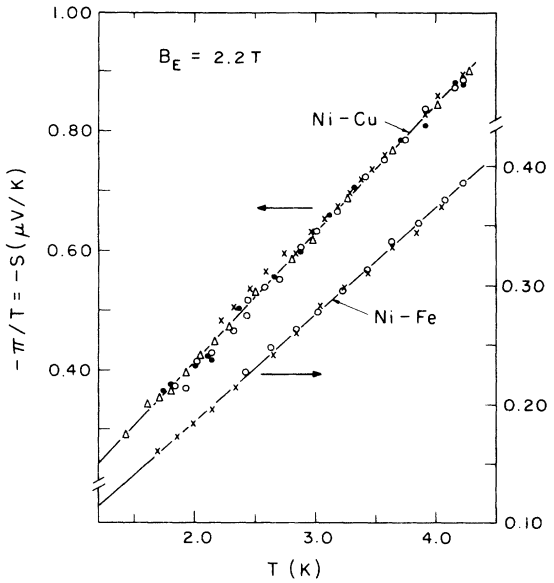

FIG. 3. Peltier effect in $Ni_{66}Cu_{34}$ and $Ni_{69}Fe_{31}$ as a function of temperature, for a fixed external field $B_E = 2.2$ T. The various symbols indicate data points obtained on different days. The solid lines have been fitted by least squares to the data.

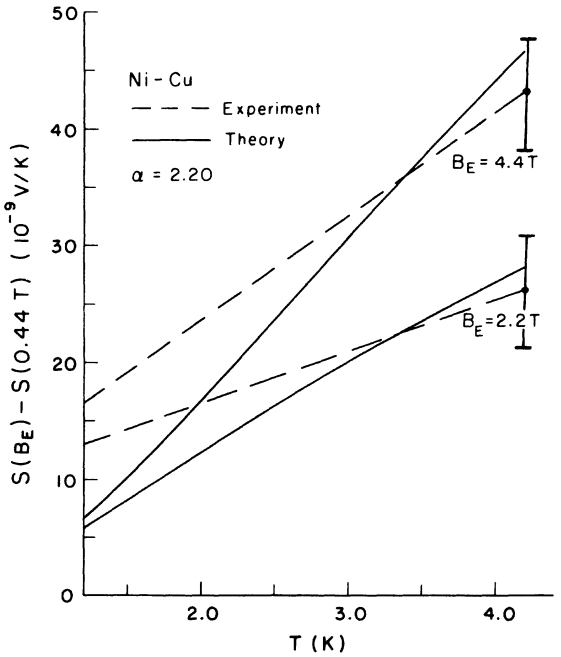

FIG. 4. Variation of $S = \pi/T$ for $Ni_{66}Cu_{34}$ between two specified external fields, above saturation.

in order to remove the effect of this variation, we show $-\pi/T^2$ in Fig. 5. Here also, $|\pi|$ is seen to decrease by about 8% above saturation. In addition, the fast decrease of $|\pi|$ below saturation ($B_E < 0.1$ T) owing to the ferromagnetic anisotropy of π is also visible. Our negative values of $S = \pi/T$ agree in sign and even in magnitude with existing data[21] for Ni-Cu alloys in zero field at low temperatures.

The electrical resistivity ρ was measured between $B_E = 0$ and $B_E = 6.6$ T, at a constant temperature of 4.2 K (Fig. 6). Since the alloy is in the residual resistance region, ρ is practically independent of temperature. A small linear decrease[22] with field is observed above saturation, which is probably caused by Pauli paramagnetism. A large increase of 2.5%, caused by the ferromagnetic anisotropy of resistivity,[3] is seen below saturation. Figure 6 shows that a field $B_E = 0.11$ T is sufficient to saturate this sample.

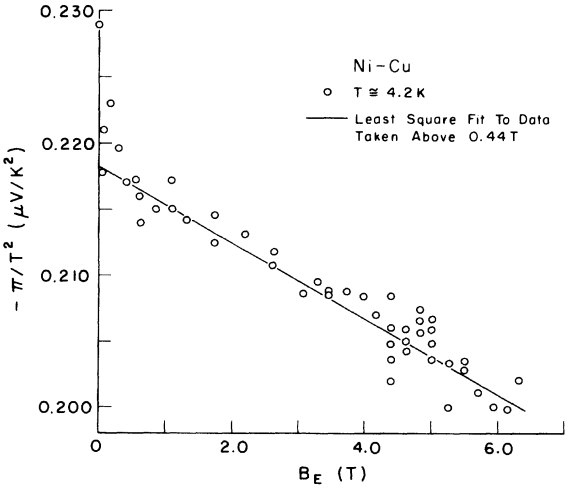

FIG. 5. Peltier effect in $Ni_{66}Cu_{34}$ as a function of external field, for a fixed temperature of 4.2 K.

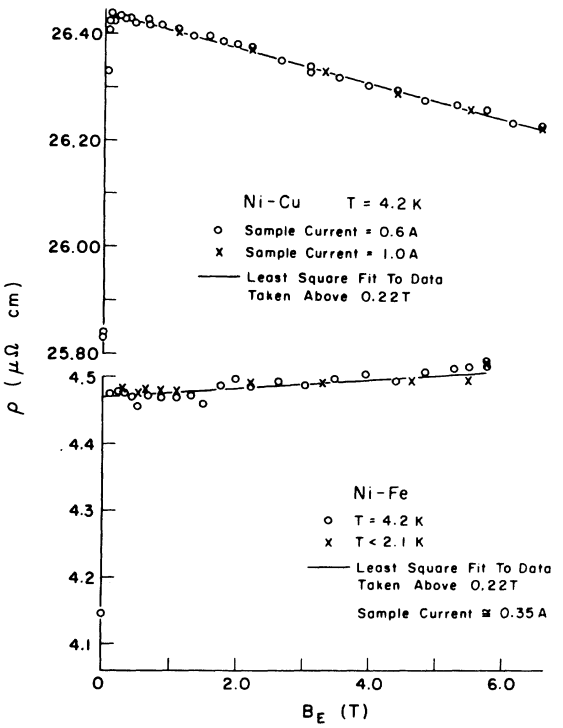

FIG. 6. Electrical resistivity of $Ni_{66}Cu_{34}$ and $Ni_{69}Fe_{31}$ as a function of external field.

VII. Ni-Fe EXPERIMENTAL RESULTS

The coefficient π was measured as a function of T at $B_E = 0$, 0.55, 1.1, 2.2, and 5.5 T, between 1.3 and 4.2 K. The data for 2.2 T are shown in Fig. 3. As for the Ni-Cu sample, we find roughly $\pi \propto T^2$, and π is negative. However, since the magnitude of π is smaller by a factor of 2 the measurements are more difficult. Hence the ac voltage exciting the thermometer bridge has to be increased from 10 to 30 mV. Also, the bridge output is fed to a digital voltmeter, rather than to a recorder.

The same method of data analysis is used as for Ni-Cu. The dashed lines on Fig. 7 show the variation of $S = \pi/T$ between two specified field values, above saturation.

Attempts to measure π as a function of field, at constant T, resulted in excessive dispersion of the data points.

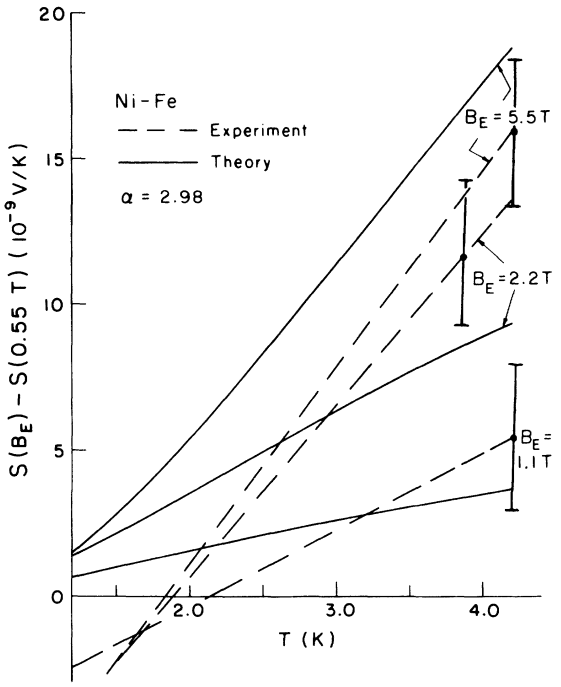

FIG. 7. Variation of the Peltier effect of $Ni_{69}Fe_{31}$ between two specified fields above saturation.

Our values of $S = \pi/T$ agree in sign and even in magnitude with available zero-field data[23] for Ni-Fe below 4 K.

The electrical resistivity was measured as a function of field between 0 and 5.7 T, at constant temperature. The current was 0.35 A. The data obtained at 4.2 and below 2.1 K do not differ appreciably (Fig. 6). A small linear increase with field is observed above saturation.[24] A large increase of about 8%, associated with the ferromagnetic anisotropy of resistivity,[3] happens below saturation. Figure 6 shows that saturation is already achieved for $B_E = 0.11$ T.

VIII. MAGNON-DRAG INTERPRETATION

The most important feature of our experimental data is the sizable dependence of π on field, above saturation (dashed curves on Figs. 4, 5, and 7). We can explain this in terms of the destruction of the magnon-drag contribution by the external field. On the basis of Eq. (7), and with the help of Eqs. (3), (6), and (8), the magnon-drag theory yields the solid curves on Figs. 4 and 7, where the constant value of the parameter α_m giving the best fit between experiment and theory is $\alpha_m = +2.20$ in the case of $Ni_{66}Cu_{34}$ and $\alpha_m = +2.98$ in the case of $Ni_{69}Fe_{31}$. That fit is rather good for $Ni_{66}Cu_{34}$. Even in the case of $Ni_{69}Fe_{31}$, the fit is no worse than the experimental uncertainty, indicated by error bars on Figs. 4 and 7. We assume $g = 2.3$, $D = 2.0 \times 10^{-40}$ J m^2, $1/n_e e = 2.3 \times 10^{-10}$ m^3/C, and $M_s = 0.2$ T for $Ni_{66}Cu_{34}$,[25-28] and $g = 2.14$, $D = 3.83 \times 10^{-40}$ J m^2, $1/n_e e = 2.0 \times 10^{-10}$ m^3/C, and $M_s = 1.36$ T for $Ni_{69}Fe_{31}$.[25,29,30]

It is comforting that these experimental values of α_m are positive and of the order of unity. The magnon-drag theory of Gurevich and Korenblit[31] predicts $\alpha_m = +1$, assuming that magnon-electron collisions are dominant and that Umklapp processes are neglected. Their theory is not very realistic since it neglects the existence of the momentum gap between spin-up and spin-down electrons at the Fermi level.

We have calculated α_m in the presence of the momentum gap, using a model appropriate for alloys, and assuming the isotropic s-d exchange interaction is active. We consider the simplest possible scattering event, where an electron is scattered and its spin flipped, and where a magnon is created or annihilated [Figs. 8(a) and 8(b)]. If momentum is to be conserved in that spin-flip process, the magnon must have a large enough wave vector to cross the momentum gap[5,32] between spin-up and spin-down Fermi surfaces. This is impossible for thermal magnons below 4 K, in the case of pure metals. However, in the case of alloys, the limited electron mean free path Λ_e implies a smearing $\Delta k = 1/\Lambda_e$ of the momentum distribution of an electron state. This leads[5] to partial overlap of the distributions for spin-up and spin-down electrons, as shown in Fig. 8(c). Electron-magnon collisions become possible. We assume a large momentum gap $|k_F^+ - k_F^-| \gg q$, $1/\Lambda_e$, and $\hbar v_F/\Lambda_e \gg k_B T$. At $T < 4$ K, we can safely neglect Umklapp processes. Assuming spherical Fermi surfaces, we obtain, finally, $\alpha_m = +1$. Thus we see that the magnon gas drifts at the same speed as the electron gas. We have proved this result in the case where the smearing $\Delta k = 1/\Lambda_e$ of the electron momentum is essential in bridging the gap. Since this uncertainty Δk is often comparable to $|\vec{q}|$, intuition might have indicated, incorrectly, that the magnon gas would not drift at all.

There also exists a collision process[32] in which the electron spin is not flipped when the magnon is created or annihilated. Since the electron is scattered between two points of the same Fermi surface, there is no momentum gap to be bridged. However, since the total spin of the crystal is not conserved in such a process, the isotropic exchange interaction between conduction electrons and magnetic localized electrons cannot be responsible for this process. As we pointed out in our earlier publication,[5] the anisotropic exchange interaction between these electrons, which exists at any given point of the Fermi surface of conduction

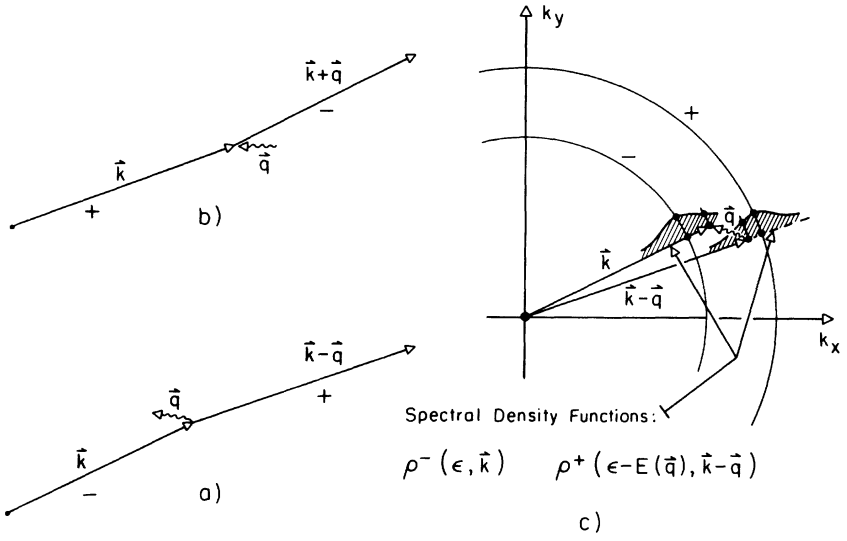

FIG. 8. (a), (b) Spin-flip processes for magnon-electron scattering. (c) Smearing of the momentum distributions of electrons by impurity scattering. The symbols + and − refer to the Fermi surfaces for spin-up and spin-down.

electrons, is the strongest interaction having the properties required to cause this kind of process. It predicts a magnon relaxation rate $1/\tau_m \propto \omega/q \propto \omega^{1/2}$ in the clean limit $\Lambda_e q \gg 1$, and $1/\tau_m \propto \omega\Lambda_e \propto \omega/\rho$ in the dirty limit $\Lambda_e q \ll 1$. It also gives rise to magnon-drag effects. The result $\alpha_m = +1$ can also be derived for this interaction,[33] for $\Lambda_e q \ll 1$ as well as for $\Lambda_e q \gg 1$.

It may seem puzzling that our experimental α_m values are somewhat larger than +1. This may be related to the inadequacy of the one-band model. In order to evaluate the electron drift velocity $d\vec{v}_e$ coming into the definition of α_m [Eqs. (1)], we have used values of $1/n_e e$ derived from Hall-effect data.[27,29] In transition metals, electrons on various sheets of the Fermi surface may have widely different mobilities. It is well known[27,29] that the Hall effect involves preferentially electrons of high mobility and strong 4*s* character, rather than those of 3*d* character. Our large α_m values suggest that the magnon-drag Peltier effect is even more selective. Apparently, only electrons with highest mobility and strongest 4*s* character are able to collide with magnons.

The gap is the smallest, and thus the overlap the largest, in the case of electrons having the strongest 4*s* character. Hence it is these electrons which are expected to collide most often with magnons, at least through the spin-flip process.

Considering also the reasonable fit between experimental and theoretical curves for $Ni_{66}Cu_{34}$ (Fig. 4), we conclude that magnon drag gives a satisfactory explanation of our experimental data for this alloy. The situation is not so clear (Fig. 7) in the case of $Ni_{69}Fe_{31}$, where the field variation of π is smaller (4%) above saturation and more affected by experimental uncertainties.

The idea that magnon-electron scattering is the dominant process for magnon relaxation is generally consistent with our experiments on heat conduction by magnons in Ni-Fe alloys[5] and in Fe-Co alloys,[6] and with existing data on ferromagnetic resonance linewidth in Fe, Ni, and Co.[34,35]

Blatt, Flood, Rowe, Schroeder, and Cox observed a peak in the zero-field thermopower of pure iron around 200 K.[36] Moreover, the data below the temperature of the peak could be fitted to $S = F_1 T + F_2 T^{3/2}$. They attributed this behavior to magnon drag. However, if we compare their term $F_2 T^{3/2}$ to Eq. (3), and if we assume a rough value of n_e corresponding to one electron per atom, we find $|\alpha_m| \simeq 60$. This is much larger than the value $|\alpha_m| = 1$ predicted by magnon-drag theory, thus casting doubt on the magnon-drag interpretation in that case. Note that the small difference between the exponents of the T and the $T^{3/2}$ terms tends to increase the difficulty of their separation from experimental data.

IX. CONCLUSIONS AND FINAL REMARKS

We have observed a field variation of the Peltier coefficient of the alloy $Ni_{66}Cu_{34}$ above ferromagnetic saturation. This variation of about 8% probably represents the magnon-drag contribution, which is gradually destroyed by the magnetic field.

In that Ni-Cu alloy, the magnon gas is found to drift at a speed comparable with the drift speed of the charge carriers. This indicates that magnon-electron scattering is dominant over other

magnon relaxation processes. A similar field variation of the Peltier coefficient has been observed in $Ni_{69}Fe_{31}$, but the magnon-drag interpretation is not so convincing in that case.

Concentrated alloys are suitable materials for these experiments because one needs to know that large magnetic fields have no influence on the conduction electrons and thus on the electron-diffusion part of the Peltier effect.

---

*Work supported by the NSF and by the Army Research Office, Durham, N. C.

[1]D. K. C. MacDonald, *Thermoelectricity* (Wiley, New York, 1962); T. C. Harman and J. M. Honig, *Thermoelectric and Thermomagnetic Effects and Applications* (McGraw-Hill, New York, 1967); R. D. Barnard, *Thermoelectricity in Metals and Alloys* (Wiley, New York, 1972); M. V. Vedernikov, Adv. Phys. 18, 337 (1968); R. P. Huebener, in *Solid State Physics*, edited by H. Ehrenreich, F. Seitz, and D. Turnbull (Academic, New York, 1972), Vol. 27.

[2]J. M. Ziman, *Electrons and Phonons* (Oxford U.P., Cambridge, England, 1960).

[3]J. P. Jan, in *Solid State Physics*, edited by F. Seitz and D. Turnbull (Academic, New York, 1957), Vol. 5.

[4]M. Bailyn, Phys. Rev. 126, 2040 (1962); L. E. Gurevich and G. M. Nedlin, Zh. Eksp. Teor. Fiz. 45, 576 (1963) [Sov. Phys.-JETP 18, 396 (1964)]; L. É. Gurevich and I. Ya. Korenblit, Fiz. Tverd. Tela. 6, 2471 (1964) [Sov. Phys.-Solid State, 6, 1960 (1965)]; M. Roesler, Phys. Status Solidi 7, K75 (1964); C. M. Bhandari and G. S. Verma, Nuovo Cimento B 60, 249 (1969).

[5]W. B. Yelon and L. Berger, Phys. Rev. B 6, 1974 (1972).

[6]Y. Hsu and L. Berger, AIP Conf. Proc. 24, 176 (1974).

[7]G. N. Grannemann and L. Berger, *Proceedings of the International Conference on Magnetism, Moscow, August 1973* (Nauka, Moscow, 1974), Vol. 6, p. 227.

[8]A. Quattropani [Phys. Kondens. Mater. 1, 125 (1963)] has shown that this simple drifting magnon distribution leads to mathematical divergences for small magnon wave numbers. However, these divergences are removed by any small magnetic field or anisotropy field. See J. Callaway and R. Boyd, Phys. Rev. 134, A1655 (1964); P. Erdos, *ibid.* 139, A1249 (1965).

[9]C. Kittel, *Quantum Theory of Solids* (Wiley, New York, 1963), p. 55.

[10]See the appendix of Ref. 5. The expansion parameter is erroneously stated there to be M_s/B instead of $g\mu_B M_s/k_B T$.

[11]A. T. Fiory and B. Serin, Phys. Rev. Lett. 16, 308 (1966); H. J. Trodahl, Rev. Sci. Instrum. 40, 648 (1969); H. J. Trodahl and F. J. Blatt, Phys. Rev. 180, 706 (1969).

[12]J. B. Sousa, Cryogenics 8, 105 (1968).

[13]Model C200P, manufactured by Samaris, Inc.

[14]H. W. Sommers, Rev. Sci. Instrum. 25, 359 (1954).

[15]S. C. Moss, Phys. Rev. Lett. 23, 381 (1969).

[16]S. Legvold, D. T. Peterson, P. Burgardt, R. J. Hofer, B. Lundell, T. A. Vyrostek, and H. Gartner, Phys. Rev. B 9, 2386 (1974).

[17]B. Mozer and D. T. Keating, Phys. Rev. 175, 868 (1968); S. C. Moss, Phys. Rev. Lett. 23, 381 (1969).

[18]J. Jach, R. J. Borg, and D. Y. F. Lai, J. Appl. Phys. 42, 1611 (1971).

[19]J. S. Kouvel and J. B. Comly, Phys. Rev. Lett. 24, 598 (1970).

[20]C. J. Adkins, J. Sci. Instrum. 38, 305 (1961).

[21]T. Farrell and D. Greig, J. Phys. C 3, 138 (1970); J. S. Touger and M. P. Sarachik (unpublished).

[22]O. S. Galkina and L. A. Chernikova, Zh. Eksp. Teor. Fiz. 38, 3 (1960) [Sov. Phys.-JETP 11, 1 (1960)]; K. P. Belov and A. V. Pedko, Zh. Eksp. Teor. Fiz. 33, 815 (1958) [Sov. Phys.-JETP 6, 628 (1958)].

[23]See Fig. 1 of M. C. Cadeville and B. Loegel, J. Phys. F 3, L115 (1973).

[24]However, J. Smit [Physica (Utr.) 17, 612 (1951)] reports a zero slope at 20 K, for Ni-Fe containing up to 30-wt% Fe.

[25]G. I. Rusov, V. G. Pyn'ko, and A. A. Nedelko, Izv. Akad. Nauk SSSR Ser. Fiz. 31, 443 (1967) [Bull. Acad. Sci. Phys. Ser. 31, 460 (1967)]; M. H. Seavey, Phys. Rev. 170, 560 (1968); R. Weber, *ibid.* 169, 451 (1968).

[26]H. Nose, J. Phys. Soc. Jpn. 16, 342 (1961); E. I. Kondorskii, V. E. Rode, and U. Gofman, Zh. Eksp. Teor. Fiz. 35, 549 (1958) [Sov. Phys.-JETP 8, 380 (1959)].

[27]F. E. Allison and E. M. Pugh, Phys. Rev. 102, 1281 (1956).

[28]S. A. Ahern, M. J. C. Martin, and W. Sucksmith, Proc. R. Soc. Lond. 248, 145 (1958).

[29]S. Foner, Phys. Rev. 99, 1079 (1955).

[30]R. M. Bozorth, *Ferromagnetism* (Van Nostrand, New York, 1951).

[31]See Eq. (13) of L. É. Gurevich and I. Ya. Korenblit, Ref. 4.

[32]E. A. Turov, in *Ferromagnetic Resonance*, edited by S. V. Vonsovskii (Israel Program for Scientific Translations, Jerusalem, 1964).

[33]L. Berger (unpublished).

[34]S. M. Bhagat and M. S. Rothstein, J. Phys. (Paris) 32-C1, 777 (1971).

[35]S. M. Bhagat and P. Lubitz, Phys. Rev. B 10, 179 (1974); S. M. Bhagat and H. O. Stevens, J. Appl. Phys. 39, 1067 (1968).

[36]F. J. Blatt, D. J. Flood, V. Rowe, P. A. Schroeder, and J. E. Cox, Phys. Rev. Lett. 18, 395 (1967).